Physical and biological coupling in eddies in the lee of the South-West Indian Ridge

Isabelle Jane Ansorge, E. A. Pakhomov, S. Kaehler, J. R. E. Lutjeharms, J. V. Durgadoo

Abstract
Eddies have some decisive functions in the dynamics of the Southern Ocean ecosystems. This is particularly true in the Indian sector of the Southern Ocean, where a region of unusually high-mesoscale variability has been observed in the vicinity of the South-West Indian Ridge. In April 2003, three eddies were studied: eddy A, a recently spawned anticyclone south of the Antarctic Polar Front (APF),; eddy B, an anticyclone north of lying between the Subantarctic Front and the APF; and eddy C, a cyclone north of the APF west of the ridge. Elevated concentrations of total Chl-*a* coincided with the edges of the cyclonic eddy, whereas both anticyclonic eddies A and B were characterised by low total Chl-*a* concentrations. Biologically, the two anticyclonic eddies A and B were distinctly different in their biogeographic origin. The zooplankton community in the larger anticyclonic eddy A was similar in composition to the Antarctic Polar Frontal Zone (APFZ) community with an addition of some Antarctic species suggesting an origin just north of the APF. In contrast, the species composition within the second anticyclonic eddy B appeared to be more typical of the transitional nature of the APFZ, comprising species of both subantarctic and subtropical origin and thus influenced by intrusions of water masses from both north and south of the Subantarctic Front. Back-tracking of these features shows that the biological composition clearly demarcates the hydrographic origin of these features.

Introduction
Regions of high-mesoscale variability in the Southern Ocean correlate closely with the core of the flow of the Antarctic Circumpolar Current (ACC) (Lutjeharms and Baker *1980*), or where the ACC interacts with prominent bottom topography (Schulman *1975*) such at the Crozet and Kerguelen Plateaux (Gille *2003*). Altimetric and hydrographic data (Ansorge and Lutjeharms *2003*; Froneman et al. *2003*) have been used to identify an additional region of high variability in the vicinity of the South-West Indian Ridge. A recent multi-beam investigation of the South-West Indian Ridge (Sclater et al. *2005*) has shown that a series of fractures: the Du Toit, Andrew Bain, Marion and Prince Edward, cross cut this ridge between 25°E and 35°E: Hydrographic data collected during the SWINDEX (South-West Indian Ocean Experiment) surveys in 1993 and 1995 have shown that close to the South-West Indian Ridge the ACC splits into several branches (Pollard and Read *2001*) resulting in enhanced eddy generation in the lee of the ridge. Indeed, this region of high variability extends eastwards from 30°E towards the Prince Edward Islands at 37°E (Ansorge and Lutjeharms *2003*). At 30°E, the ACC transport is concentrated within the Subantarctic Front (SAF) and the Antarctic Polar Front (APF). At the ridge, these fronts are close together, suggesting that a large part of the ACC flux is constrained by the complex nature of the South-West Indian Ridge. On approaching this ridge, there is a noticeable separation in the two branches of the ACC with the SAF topographically deflected north-eastwards, thus widening the Antarctic Polar Frontal Zone (APFZ) by up to 5° of latitude (Fig. 1). These observations are consistent with Belkin and Gordon's (*1996*) study of the frontal regions in the Indian Ocean, which document for the first time the separation of the SAF-APF as a result of the northward deflection of the SAF upstream of this ridge. Of interest is the fact that both studies differ from Pollard et al. (*2007*) who have shown that although the SAF crosses over the South-West Indian Ridge, it passes south of the Del Caño Rise between 47°S–48°S and ~46°E–48°E before turning sharply north upstream of the Crozet Archipelago. The apparent contradiction between these two concepts may be resolved by the addition of a Southern SAF (SSAF) formed as the SAF splits at the South-West Indian Ridge and passes southwest of the Prince Edward Islands (Froneman et al. *2003*). Thus, the SAF identified by Pollard et al. (*2007*) may in fact be the SSAF. It is also interesting to note that extensive XBT transects south of New Zealand (Budillon and Rintoul *2003*) have shown a similar pattern with the SAF bifurcating to form a northern (6°C, at 200 m) and a southern (3.5°C, at 200 m) branch as a result of the topographical influence of the Macquarie Ridge. Based on all these findings, it has been surmised that the funnelling of the greater part of the ACC through the fractured South-West Indian Ridge in this region is the main cause for the generation of several branches within each frontal band as well as cyclonic and anticyclonic eddies. However, the hydrographic and dynamic characteristics of these eddies close to their source remain

poorly understood, and while the importance of these eddies as foraging grounds for grey-headed albatrosses (Nel et al. *2001*) has been documented, there is still very limited understanding of their importance in the life-support system of the nearby Subantarctic Islands. Previous studies conducted upstream of the Prince Edward Islands have not revealed any spatial patterns of distribution in either surface or depth-integrated Chl-*a* as well as in mesozooplankton density and composition (Bernard and Froneman *2002*, *2005*). The waters around the Prince Edward Islands are situated within an eddy-rich environment (Ansorge et al. *2006*) and consequently known for their mixed plankton communities and diverse biogeography. Antarctic, Subantarctic and even Subtropical species have all been recorded in the vicinity of these islands (e.g. Boden *1988*). However, only one study has investigated the biogeography of a cold eddy formed close to the South-West Indian ridge (Bernard et al. *2007*). In their findings, Bernard et al. (*2007*) have linked significant differences in the macroplankton composition both inside and outside of the eddy to its point of origin.
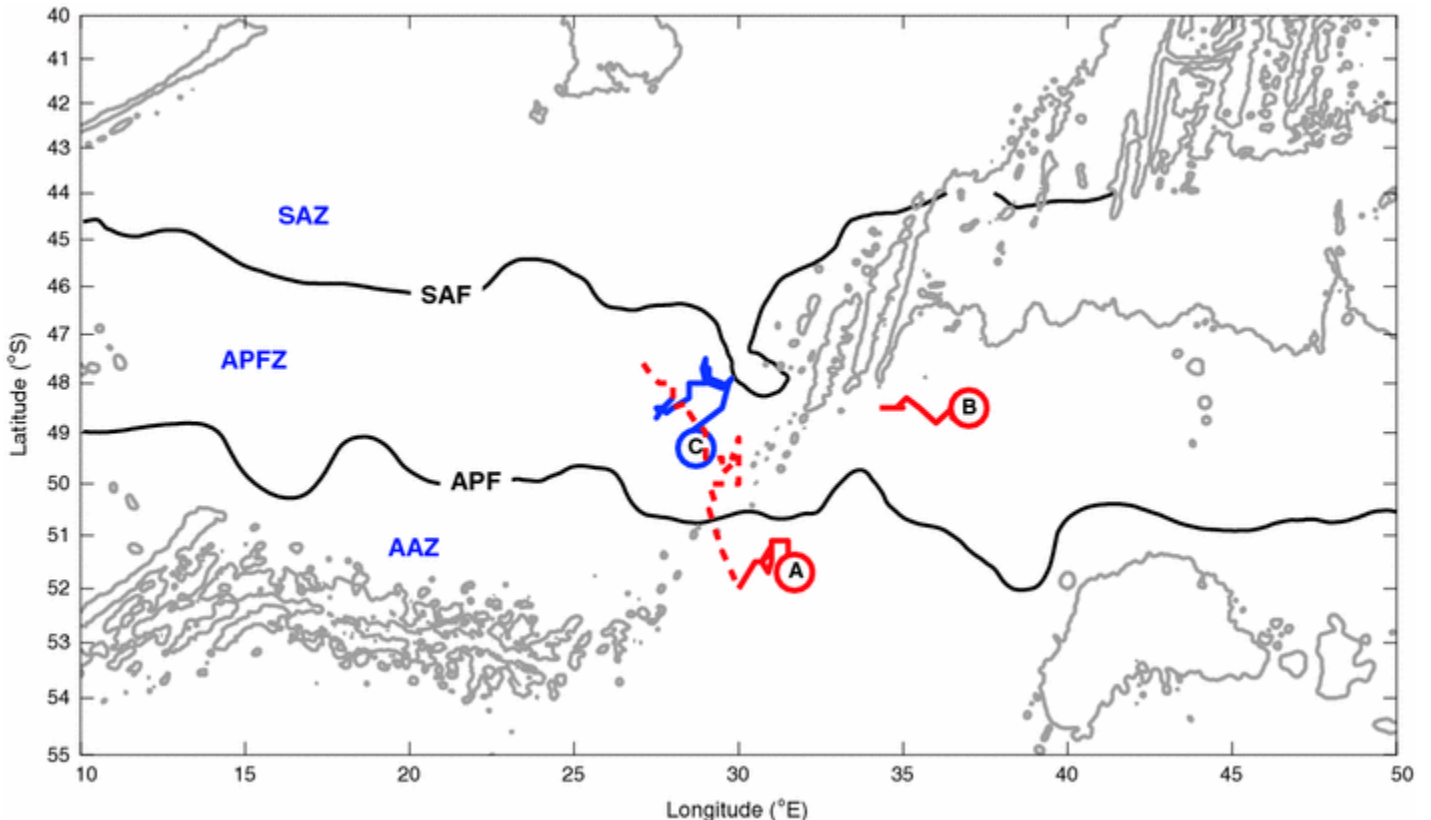

Fig. 1 A schematic showing the mean position of the subsurface (200 m) expression of the Subantarctic Front (SAF) (6°C isotherm) and the Antarctic Polar Front (APF) (2°C isotherm). The position of eddies **a**, **b** and **c** in relation to the SAF and APF and their trajectories leading up to the survey in April 2003 are represented by a *solid line*. Of interest is the trajectory of eddy A, which splits from a parent into a child eddy (*dashed line*) in January 2003. The 4,000-m isobath is shown. *SAZ* Subantarctic Zone, *APFZ* Antarctic Polar Frontal Zone, *AAZ* Antarctic Zone

To date, this region of increased oceanographic activity coupled with its influence on the plankton community structure has received not much attention. The main objective of the DEIMEC II cruise, therefore, was to investigate the nature of eddies formed upstream of the Prince Edward Islands in their ambient hydrographic environment. In addition, the biological content of these eddies, with a particular interest to Chl-*a* distribution and macroplankton/micronekton composition, has also been studied. The emphasis on the low and high levels of the food web was partially dictated by the limited survey time, absence in the mesozooplankton differences in previous studies and macroplankton/micronekton importance for the top predators. The hypothesis that all these eddies are formed exclusively at the South-West Indian Ridge is not entirely satisfying because some

enhanced mesoscale variability is also found west of the ridge at 25°E (Ansorge et al. *2006*). The opportunity to investigate at least two of these upstream eddies, therefore, was high on the list of priorities for the cruise.

Methodology
Identification of eddies from altimetry data
Specific anomalies were tracked manually in the region of the South-West Indian Ridge by identifying them at regular space and time intervals. The wide ground track observations of the TOPEX/Poseidon mission south of South Africa (Gründlingh *1995*) have led to discontinuity in the eddy tracking process, resulting in extensive extrapolation to establish continuity in eddy course. However, the probability of anomalies "disappearing" or "reappearing" while drifting across satellite tracks are greatly lessened by the combination of dual satellite crossovers of TOPEX/Poseidon and Jason-1 with the closely spaced ground tracks of ERS-2. Consequently, one can be more confident of the continuity in the passage of either cyclonic or anticyclonic anomalies from one period to another (Ansorge and Lutjeharms *2003*). Thus it was assumed that an intense anomaly (>35 cm) (henceforth referred as eddy A), located near the point of formation between 50°S–52°S and 29°E–33°E, represented a newly generated (formed January 2003) anticyclonic eddy (Fig. 2). SSH data clearly show that while this eddy had been formed in January 2003, it had in fact split from a "parent" eddy which had relocated south-eastwards into the vicinity of the South-West Indian Ridge between June and December 2002 (Fig. 1). Further to the north-east at 48°30′S and 36°E, a weaker positive anomaly (~25 cm) (henceforth referred as eddy B) was identified as an eddy that had been formed prior to the cruise in the APFZ and thus represented the transitional nature of this region (Fig. 2). A negative anomaly (henceforth referred as eddy C) its SSH measuring −40 cm was observed between 48°30′S–50°15′S and 28°E–29°30′E (Fig. 2).
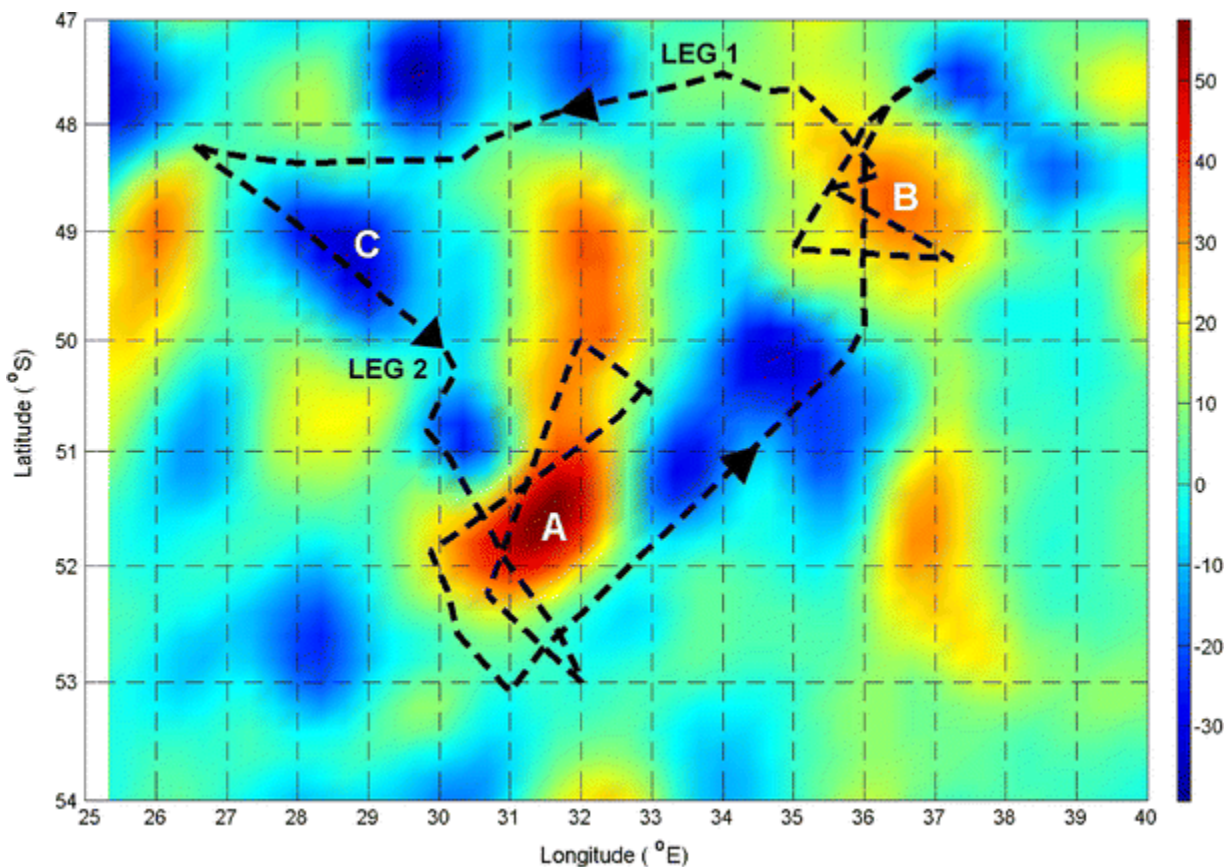

Fig. 2 Sea surface height in cm (SSH) for 9 April 2003 showing the location of all three eddies (**a**, **b**, **c**) surveyed. Overlaid onto the SSH field is the cruise track occupied during this period. The location of legs 1 and 2 is shown

A full CTD (conductivity–temperature–depth) study of the cold eddy in the north-western region had to be curtailed due to storm conditions and only underway thermosalinograph and XBT (expendable bathythermograph) data were obtained across this feature. Hence, two anticyclones generated in the vicinity of the South-West Indian Ridge and within the APFZ have been studied in detail and a cyclone only partially. Observations en route to these features and in the regions between them gave information on the location of the SAF and APF at the time of the survey and are discussed in the following section. A total of 30 CTD and 71 XBT stations were undertaken en route and in the vicinity of the South-West Indian Ridge onboard the research and supply vessel *SA Agulhas* between 6 and 18 April 2003 (Fig. 2). At each CTD station, vertical profiles of salinity, temperature and density were obtained to a maximum depth of 1,000 m. Sippican T7 XBTs were deployed to a maximum depth of 760 m.

Surface seawater samples were collected at each XBT station by lowering a bucket overboard from the side of the ship as well as at five standard depths (0, 20, 50, 75 and 100 m) at each CTD station. Surface samples were always size-fractionated into micro (>20 μm), nano (2–20 μm) and pico (<2 μm) size classes by passing 250 ml seawater sequentially though 20 μm Nitex, 2 μm Nucleopore and GF/F Whatman filters, respectively. For other depths, 250 ml of seawater was filtered through a GF/F filters only (vacuum <5 cm Hg). Chl-*a* and phaeopigments were then extracted in 8 ml of 90% acetone during 24 h at −20°C. The pigment concentrations were measured using a Turner Design 700 Fluorometer, after the method of Strickland and Parsons (*1968*).

Macrozooplankton samples were collected using a rectangular mid-water trawl (RMT-8) with a nominal mouth area of 8 m^2 and mesh size of 4.5 mm. It was our intention to sample inside and outside the two positive anomalies and as far south as possible. A total of nine RMT-8 trawls were undertaken with two trawls conducted within and two outside each of the positive anomalies (eddies A and B) (Fig. 3). The trawl was towed obliquely between 0 and 300 m during darkness. Towing speed and duration varied between 2 and 3 knots and 20 and 25 min, respectively. The trawl was fitted with a universal underwater unit (U^3, Robertson et al. *1981*) that monitored continuously depth and temperature as well as the opening and closing times of the trawl. The volume filtered by the trawl was determined by multiplying the effective mouth area of the trawl by the distance travelled. This was calculated from the ship's speed and the duration the net had opened. In calculating the volume filtered, the effect of towing speed was also taken into consideration (Roe et al. *1980*). Samples were preserved in 6% buffered formalin and examined in the laboratory within 1 month of collection. Catches were sorted and analysed for taxonomic identification, numerical abundance and individual length measurements. Macroplankton abundance data were expressed as individual m^{-2}.
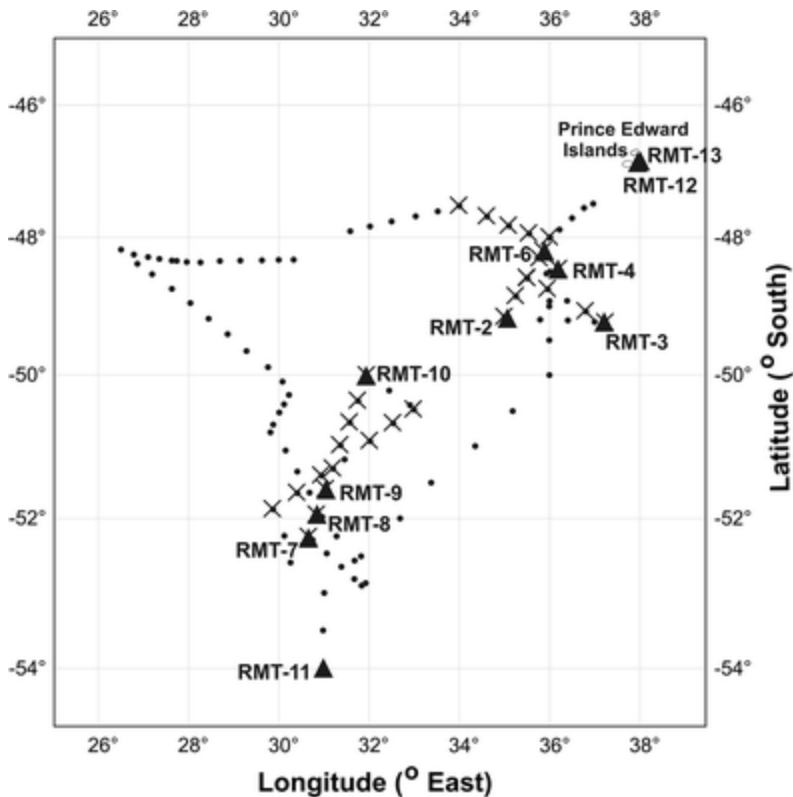
Fig. 3 Position of stations occupied during the survey. *Filled circles* XBTs and surface size-fractionated Chl-*a* and POMP; *filled triangles* Rats; *crosses* CTDs and depth-integrated total Chl-*a*

Macrozooplankton communities were investigated using PRIMER (Clarke and Warwick *1994*). Prior to all analyses, species abundances were transformed using the function $\log_{10}(x + 1)$ to reduce the weighting of highly abundant species. Following transformation, cluster analysis (*q*-type) was used to group stations based on the Bray–Curtis similarity measure and group average classification of abundance data (Field et al. *1982*). Unfortunately, sample size was too small (2–5 stations in the clusters) to conduct meaningful statistical analyses between station groups.

Results
Oceanographic setting in the vicinity of the South-West Indian Ridge during DEIMEC II
The Prince Edward Islands are located in the Indian Ocean sector of the Southern Ocean at 46°50′S 37°50′E. Intensive investigations carried out on the oceanic frontal systems south of Africa (e.g. Lutjeharms and Valentine *1984*; Lutjeharms *1985*) have shown that the islands are situated directly in the path of the ACC bounded to the south by the APF and the SAF to the north (Fig. 1). Water masses between these two fronts are transitional by nature with Subantarctic Surface Water (SASW), commonly found north of the SAF in the Subantarctic Zone (SAZ), gradually modifying with distance across the APFZ to become Antarctic Surface Water (AASW) south of the APF in the Antarctic Zone (AAZ) (Fig. 1). At the time of the survey underway XBT measurements along a westward transect between 34°30′E and 26°30′E (Leg 1) identified a meandering SAF along the northern boundary of the survey area between 48°15′S, 30°E and 48°S, 32°15′E (Fig. 4a). This transect crossed over the South-West Indian Ridge at the Prince Edward Fracture Zone and into the deep Agulhas Basin. An intense negative eddy (eddy C) with an SSH <−40 cm centred at 29°30′E was observed (Fig. 2). It was anticipated that eddy C could be studied in detail in the time available, but unfortunately, severe weather conditions hampered a complete CTD survey and only XBT measurements were made.
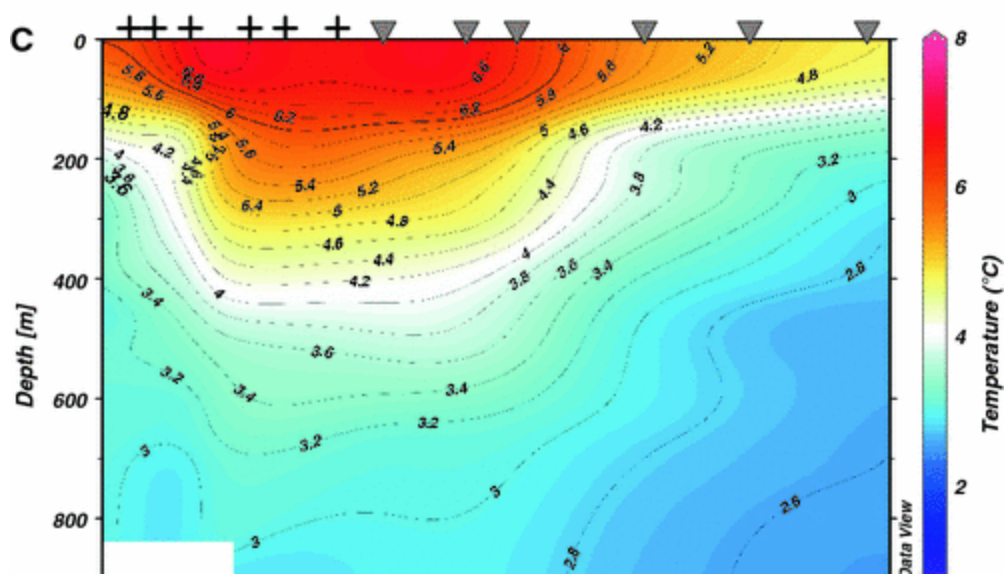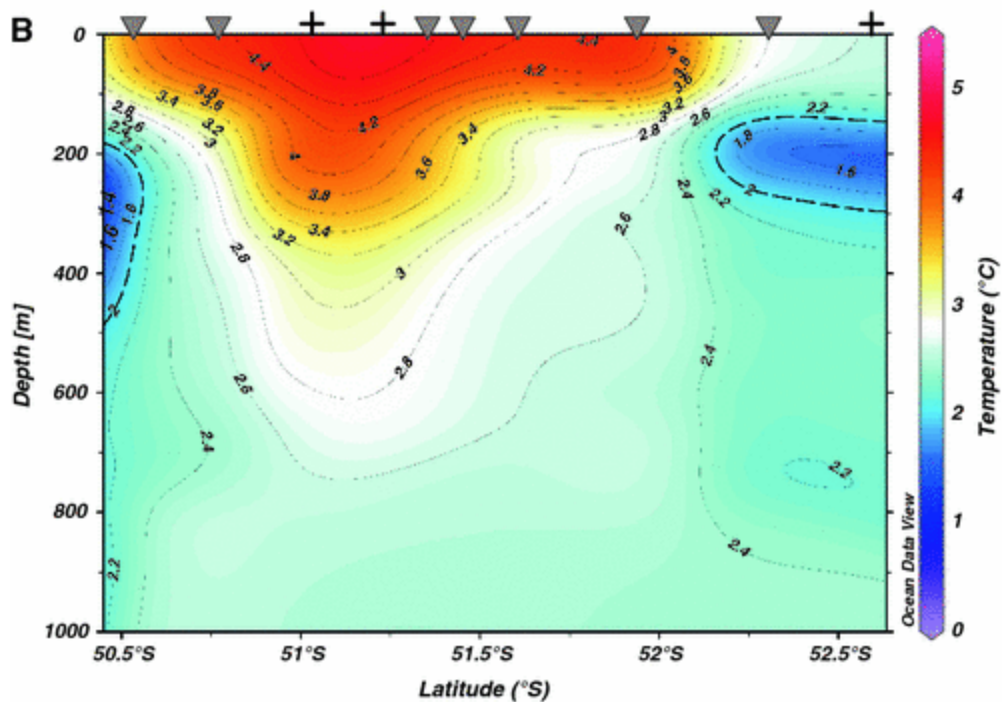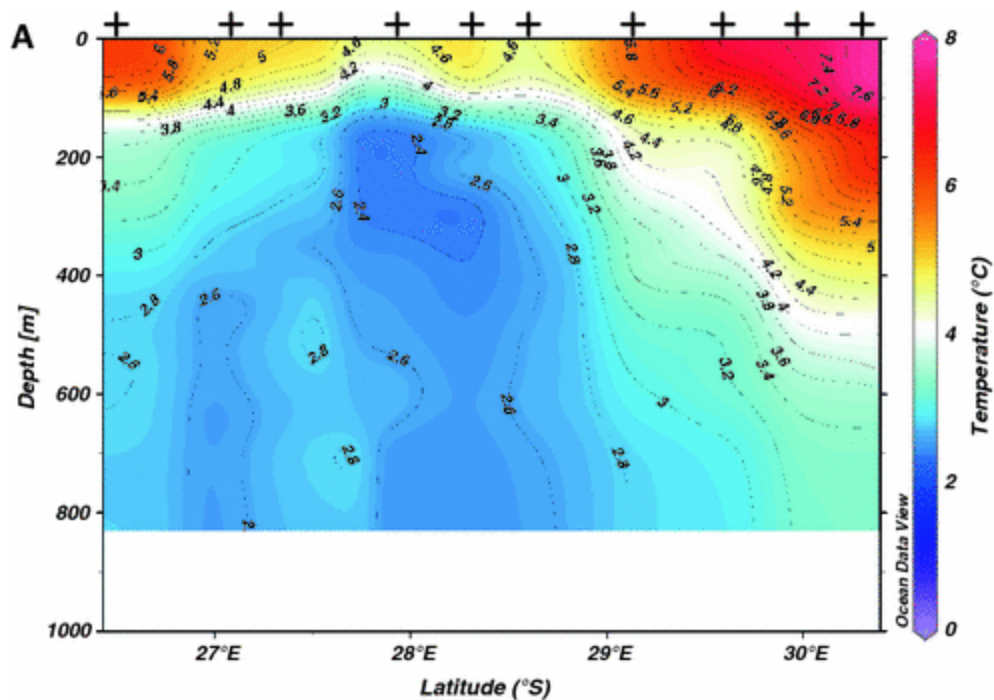
Fig. 4 Temperature sections undertaken through **a** eddy C, **b** eddy A and **c** eddy B. The temperature clearly defines the boundaries and physical characteristics of each feature. *Cross symbols* denote underway XBT stations while *inverted triangles* denote CTD stations

A second underway transect Leg 2 (between 26°30′E, 48°10′S and 32°E, 53°S), parallel to the South-West Indian Ridge was occupied enroute to the main anomaly of interest, eddy A (Fig. 2). XBT measurements enroute to this feature, crossed over the APF at 48°45′S and again at 52°S suggesting that the front meandered across the survey region—possibly steered by the occurrence of eddy A, which lay directly south of the APF. Our findings along this leg of two distinct branches associated with the APF are comparable to those presented by Park et al. (*1997*) and highlight the extreme temporal and spatial variability in frontal bands at 30°E.

Hydrography of Eddy A

Anomaly A was assumed to represent a newly formed eddy (Fig. 2) lying directly within the region of highest sea surface height (SSH) variability centred at 51°30′S, 31°E (Ansorge and Lutjeharms *2003*). Its diameter from hydrographic observations (Fig. 4b) was approximately 250 km and it extended to a depth of at least 1,000 m. The positive SSH anomaly and the strong surface temperature (1.93–5.10°C) and surface salinity (33.683–33.963) expressions across this feature, relative to its surroundings, indicates that it was a warm, anticyclonic eddy formed north of the APF (Figs. 1, 4b). Geostrophic velocities calculated from CTD data measured 0.54–0.85 ms^{-1} at the edges of this feature and further support the notion that eddy A, as the positive SSH signature suggest (Fig. 2), is indeed an anticyclonic eddy. Stations occupied within eddy A were characteristic of the APFZ. Closer examination of SSH data hints at this eddy being formed from the split of a parent eddy, which had moved south-eastwards from an original position in the APFZ of 47°45′S and 27°E (Fig. 1). Indeed, water mass composition within eddy A was typical of modified SASW (Fig. 5) found within the transitional APFZ and further corroborates the split of this eddy from a parent eddy, which had moved south across the APF. SASW extends from the surface to the depth of the Antarctic Intermediate Water (AAIW) and is characterised by a shallow subsurface salinity maximum as a result of excess precipitation over evaporation in the surface layers at these mid- latitudes. Within the eddy, the salinity maximum signature, typical of SASW, of 33.850 was found between 150 and 180 m (Fig. 5). Comparisons with a station located directly within the APFZ at 47°S and thus containing waters typical of unmodified SASW (Pakhomov et al. *2000*) show a similarity with that of the core of this eddy. Although surface water masses within eddy A were colder (~2°C) and fresher (0.13) than within the APFZ proper (Fig. 5) the similarity in profile is clear. In addition, the near Subantarctic nature of eddy A is highlighted by comparing the hydrographic characteristics of stations located within the core of the eddy and on its north-eastern and south-western extremities. Water masses within the core represent modified SASW, whereas on the outer extremities stations represent water masses typical of the Antarctic Zone (temperatures 0.6–2.94°C and salinities 33.79–34.03) indicative of the close proximity of the APF, which lay north of eddy A. AASW is characterised by a shallow temperature minimum associated with the remnants of Winter Water. Indeed, the θ/S profile of water at CTD 25 to the north of eddy A shows that water masses are typical of AASW, suggesting that the APF was forced to meander around this feature or that filaments of Antarctic water were drawn around it. Koshlyakov et al. (*1985*) have shown that water masses may become entrained by the rotation of eddies within the APFZ. Comparing station CTD 64, occupied within the AAZ proper at 53°45′S during the CIVA 2 cruise in 1996 (Park et al. *1997*), with CTD 17, located 2° of latitude to the north, draws a compelling similarity.
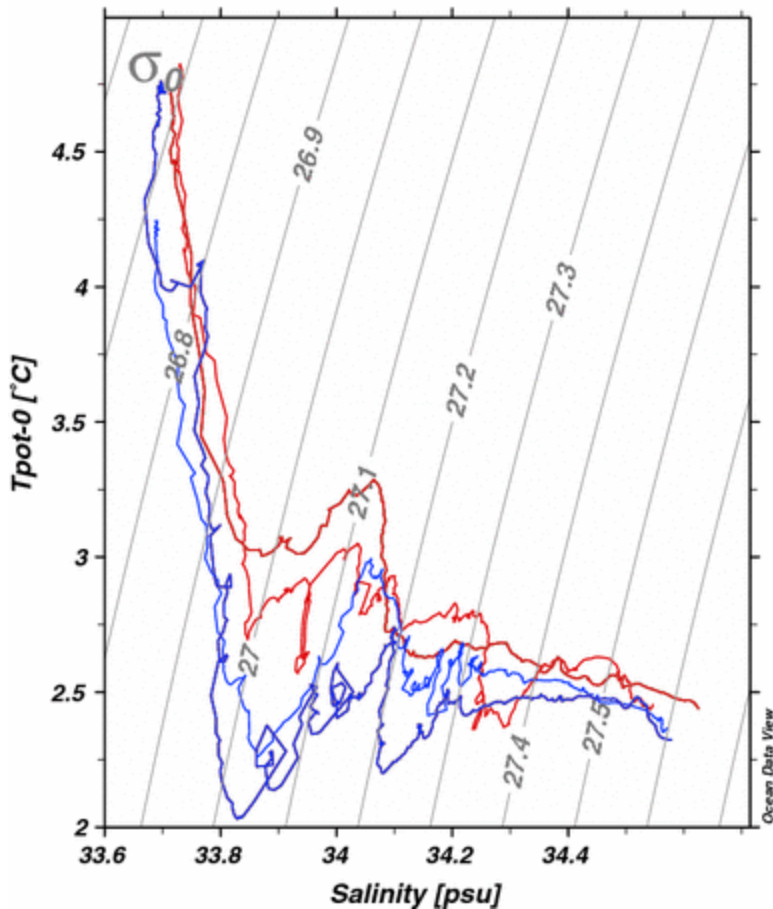
Fig. 5 θ/S plots of stations occupied within eddy A and eddy B. The similarity in profile and water mass characteristic is shown, despite these eddies being observed approx. 300-nm apart

Hydrography of Eddy B

A number of studies (e.g. Ansorge and Lutjeharms *2003*; Ansorge et al. *2006*; Swart et al. *2008*) have shown that eddies in this region exhibit specific trajectories, which may cause these features to drift towards the Prince Edward Islands. Furthermore, drifter data (Ansorge and Lutjeharms *2005*) have shown that with time and distance away from the source region that eddies gradually "spin down", becoming unrecognisable in their surface and subsurface signatures. Consequently, while eddy A, could be assumed to be newly spawned; further to the north-east a weaker positive SSH eddy, centred at 48°30′S and 36°E (eddy B), was initially thought to be an eddy of a more advanced age (Figs. 2, 4c). However, altimetry data used to track this feature for the period December 2002–April 2003 showed that this eddy had in fact formed west of its current position and drifted into the island vicinity from an original position of 48°30′S and 34°30′E (Fig. 1). Water masses within eddy B are typical of true SASW with an average temperature of 6.95°C and salinity of 33.78, and display a distinct subsurface salinity maximum of 34.21 between 190 and 200 m. CTD stations 5 and 6 were located on the south-western and south-eastern boundaries of the eddy and are typical of modified SASW similar to stations located in the core of eddy A. Comparisons between eddies A and B (Fig. 5) show that although water masses in both eddies are indicative of SASW origin, those found in eddy A were substantially fresher and cooler than those of eddy B.

To date, eddies found close to the South-West Indian Ridge have received not much research attention. To understand the effect of these particular eddies on the ecosystem of the region their role in the dynamics of the plankton community needs to be better understood.

Chlorophyll *a* distribution
Surface Chl-*a* concentrations along the cruise track were generally low ranging from 0.1 to 0.4 mg m^{-3} (Fig. 6a). The distribution of total Chl-*a* in the area investigated showed no clear pattern, except slightly elevated Chl-*a* patches (ca. 0.3–0.4 mg m^{-3}) in the north-eastern, western and southern parts of the survey (Fig. 6a). Throughout the survey, Chl-*a* was generally dominated by the pico- and nano-size fractions accounting for 75–95% of the total Chl-*a* standing stock. There was no spatial pattern in pico- and nano-Chl-*a* size fractions across the investigated area. Although microphytoplankton Chl-*a* concentrations never exceeded 0.2 mg m^{-3}, highest concentrations of this size fraction were observed in the western and southern parts of the survey (Fig. 6b). At these stations, the contribution of the micro size fraction to the total Chl-*a* standing stock increased to 35–54% often becoming the single most important size fraction. The highest total Chl-*a* and micro Chl-*a* concentrations appeared to coincide with the areas influenced by waters of the meandering APF (Figs. 6a, b). The westernmost part of the survey supported one of the highest Chl-*a*/phaeopigments ratios (8–11) observed during the cruise, suggesting the influence of Antarctic water masses enhancing productivity (Fig. 6c). In contrast, in the rest of the surveyed area (excluding the abovementioned eddies), Chl-*a*/phaeopigments ratios were generally below five (Fig. 6c). Vertical distribution (data are not shown) of total Chl-*a* was uniform in the top 100 m layer sharply decreasing below 100 m depth. As a consequence, there was good predictable agreement between surface and depth-integrated Chl-*a* levels at the CTD stations.
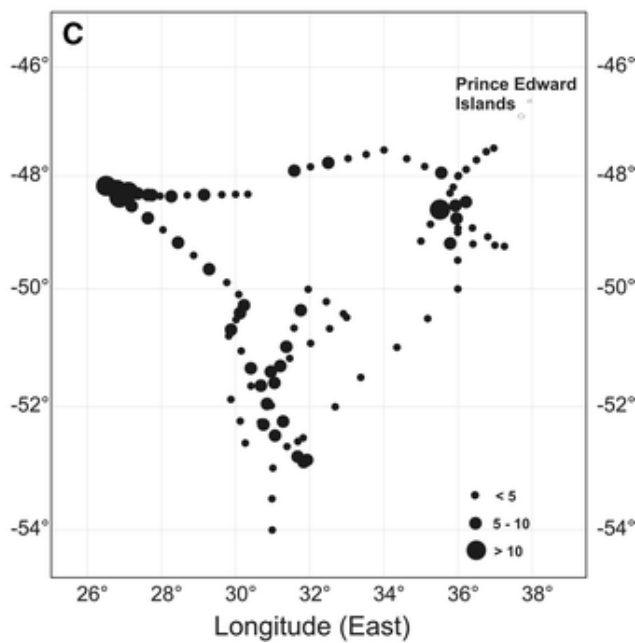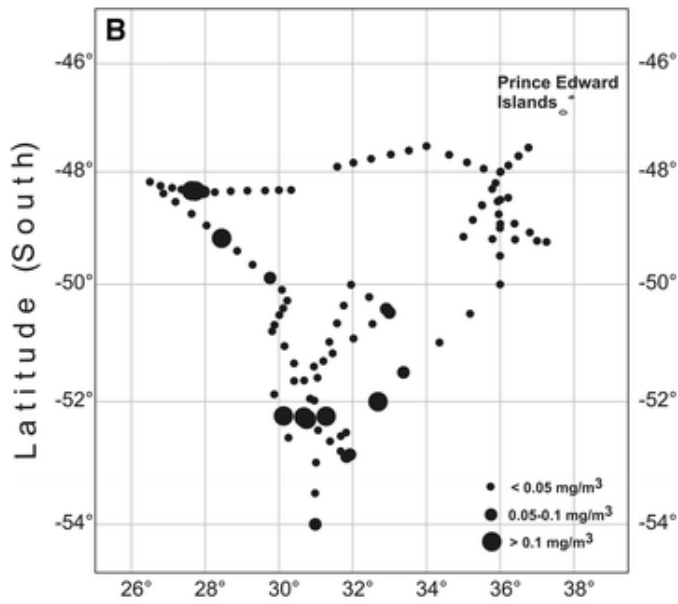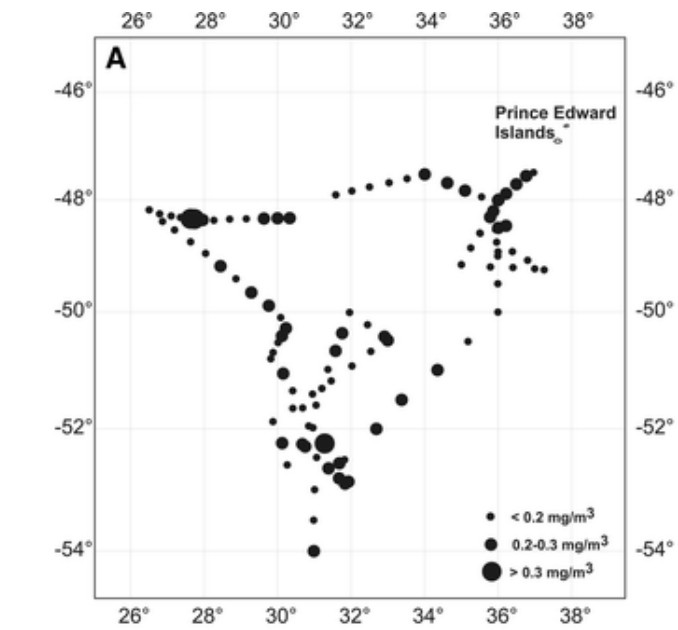
A

Prince Edward
Islands

< 0.2 mg/m^3
0.2-0.3 mg/m^3
> 0.3 mg/m^3

B

Prince Edward
Islands

< 0.05 mg/m^3
0.05-0.1 mg/m^3
> 0.1 mg/m^3

Latitude (South)

C

Prince Edward
Islands

< 5
5 - 10
> 10

Longitude (East)

Fig. 6 Spatial distribution of total Chl-*a* (**a**), micro size fraction of Chl-*a* (**b**) and Chl-*a*/phaeopigment ratios (**c**) during the DEIMEC 2 survey

Macroplankton community structure within the survey region
In total, 46 taxa were identified in the RMT-8 samples (Table 1). Fish were the most diverse group of macroplankton accounting for 14 taxa, followed by euphausiids (9 taxa), hyperiids (6) and coelenterates (6). Total abundance of macroplankton ranged between 2 and 21 ind m^{-2} in the top 300 m layer. Although fish were the most diverse group taxonomically, they contributed <16% to total macroplankton abundance. The most prominent group consisted of pelagic tunicates, namely *Salpa thompsoni*, which accounted for 29–82% of total abundance. This was followed by euphausiids (9–39%) and chaetognaths (4–17%) (Table 1).

Table 1 Densities (ind m^{-2}, ±1SD) of macrozooplankton and micronekton collected southwest of the Prince Edward Islands using the RMT-8 oblique tows in the top 300-m layer

Taxa	South of APF	Inside eddy B	Inside eddy A and outside eddies A and B
Coelenterata			
Calycopsis borchgrevinki	0	0	0.004 ± 0.009
Pegantha spp.	0	0	0.201 ± 0.285
Periphylla periphylla	0.026 ± 0.036	0	0
Hydromedusae gen sp.	0	0.060 ± 0.063	0
Amphycaryon acuale	0	0	0.091 ± 0.089
Siphonophora (unidentified)	0	0.138 ± 0.131	0.004 ± 0.009
Ctenophora			
Beroe cucumis	0.038 ± 0.053	0.063 ± 0.088	0.068 ± 0.081
Polychaeta			
Tomopteris carpenteri	0.019 ± 0.026	0	0
Tomopteridae gen sp.	0	0.008 ± 0.011	0
Mollusca			
Spongiobranchaea australis	0	0.031 ± 0.044	0
Cymbulia sp.	0	0.011 ± 0.014	0
Alluriteuthis antarcticus	0	0.031 ± 0.044	0.020 ± 0.013
Kondakovia longimana	0	0	0.013 ± 0.017
Euphausiacea			
Euphausia vallentini	0	0.537 ± 0.098	0.262 ± 0.075
Euphausia longirostris	0	2.172 ± 1.984	0.024 ± 0.032
Euphausia triacantha	0.538 ± 0.254	0	0.978 ± 0.568
Euphausia similis	0	0.280 ± 0.225	0
Euphausia frigida	0.202 ± 0.141	0	0
Thysanoessa spp. (*vicina*)	0	0.316 ± 0.151	0.082 ± 0.114
Thysanoessa gregaria	0	0.064 ± 0.027	0
Stylocheiron maximum	0	0.063 ± 0.088	0.008 ± 0.018
Nematoscelis megalops	0	0.070 ± 0.078	0

Taxa	South of APF	Inside eddy B	Inside eddy A and outside eddies A and B
Amphipoda			
Themisto gaudichaudii	0.019 ± 0.026	0.052 ± 0.073	0.138 ± 0.115
Primno macropa	*0*	*0*	*0.004 ± 0.009*
Mimonectes sphericus	0.051 ± 0.072	0	0.008 ± 0.018
Phronima sedentaria	0	0.011 ± 0.014	0
Vibilia sp.	0	0.015 ± 0.021	0.033 ± 0.033
Gammaridea gen sp.	0	0	0.007 ± 0.015
Decapoda			
Sergestes sp.	0	0.279 ± 0.374	0.008 ± 0.018
Chaetognatha			
Sagitta gazellae	0.262 ± 0.209	0.689 ± 0.504	0.381 ± 0.276
Eukrohnia hamata	0.115 ± 0.055	0.182 ± 0.215	0.242 ± 0.145
Tunicata			
Salpa thompsoni	0.649 ± 0.169	3.810 ± 0.155	12.29 ± 3.894
Osteichthyes			
Electrona antarctica	0.051 ± 0.072	0	0
Electrona carlsbergi	0	0	0.007 ± 0.015
Gymnoscopelus piabilis	0	0	0.020 ± 0.045
Gymnoscopelus braueri	0	0	0.021 ± 0.037
Gymnoscopelus nicholsi	0	0.026 ± 0.006	0
Gymnoscopelus sp.	0.103 ± 0.144	0	0
Lampanyctus intricarius	0	0.011 ± 0.014	0
Krefftichthys andersoni	0.057 ± 0.080	0	0.013 ± 0.017
Protomyctophum bolini	0.121 ± 0.118	0.011 ± 0.014	0.053 ± 0.036
Protomyctophum choriodon	0.026 ± 0.036	0	0
Myctophidae larvae	0	0.021 ± 0.029	0.007 ± 0.015
Bathylagus antarcticus	0	0	0.006 ± 0.012
Indiacanthus atlanticus	0	0.011 ± 0.014	0
Stomias boa boa	0	0	0.022 ± 0.032
Total	2.275 ± 0.333	8.958 ± 3.799	15.016 ± 4.332

The groupings were identified using cluster analysis

The hierarchial cluster analysis identified three distinct groupings of stations at the similarity level of 53% (Fig. 7a). The most distant grouping, separated at ~31% of similarity, included stations occupied south of the APF. These stations were characterised by the lowest number of species (15) and total mean abundance (2.3 ind m^{-2}). In this grouping, euphausiids, mostly *Euphausia triacantha* and *E. frigida*, predominated, accounting for ~33% of total abundance. They were followed by *S. thompsoni* (29%), chaetognaths (17%) and mesopelgic fish (16%) mostly presented by the genera *Protomyctophum* and *Gymnoscopelus* (Table 1).
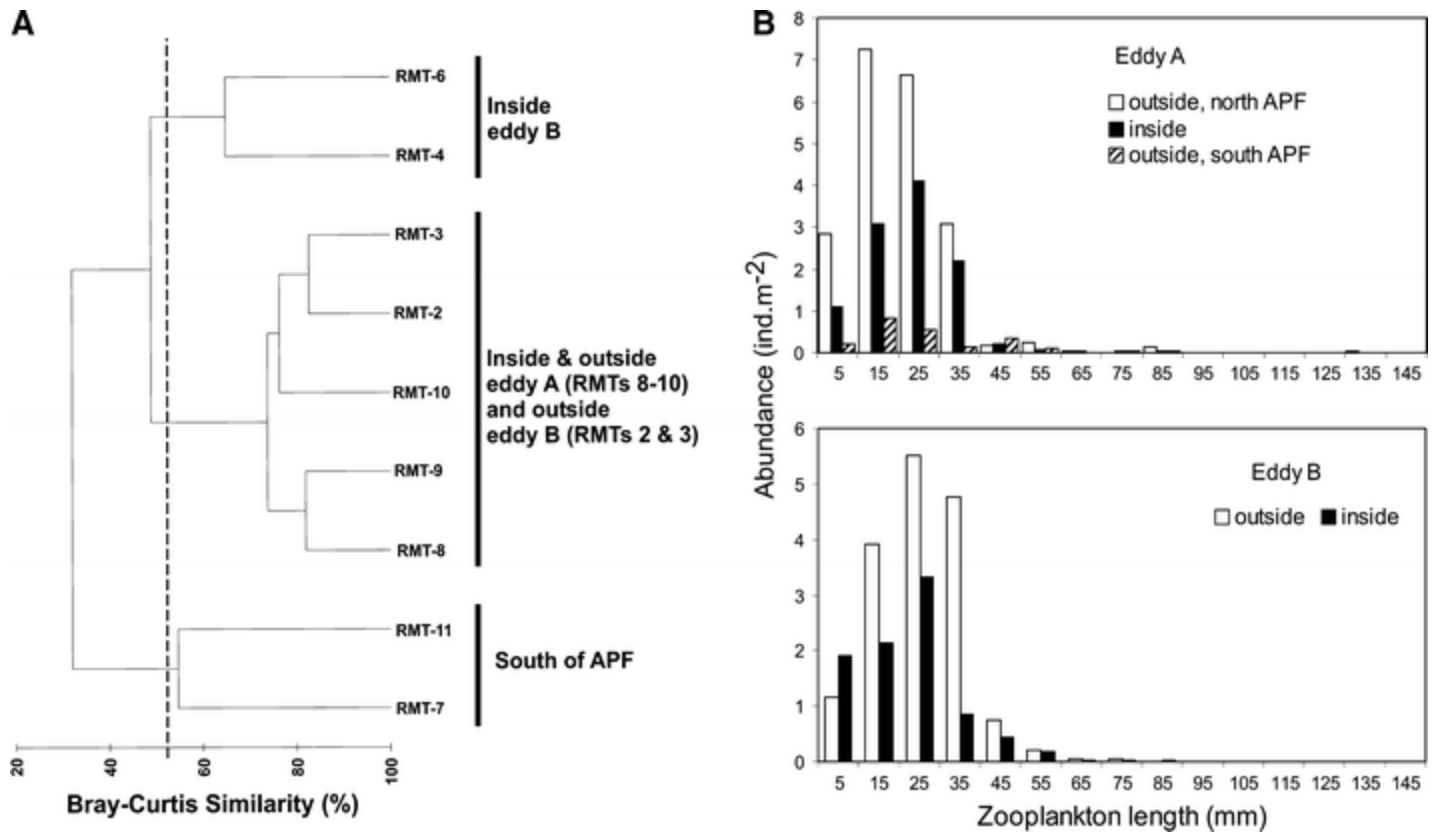
Fig. 7 **a** Dendrogram of macrozooplankton/micronekton abundance similarity matrix of stations conducted inside and outside eddies A and B during DEIMEC II cruise, **b** length–frequency of total zooplankton samples within and in adjacent waters of eddies A and B during the DEIMEC II survey

The other two groupings are separated at the ~50% similarity level. The small grouping included stations occupied inside eddy B, while the largest grouping consisted of the tight group of stations conducted inside and outside of eddy A as well as outside eddy B (Fig. 7a). The grouping of stations inside eddy B included 26 taxa and had a moderate abundance (ca. 9 ind m^{-2}, Table 1). *S. thompsoni* was the most important species in this grouping, contributing 43% to total abundance. Tunicates are closely followed by euphausiids (39%), with *E. longirostris, E. vallentini* and *Thysanoessa* spp. being the most numerous species. The third most numerous group consisted of chaetognaths (~10%).

The largest grouping of stations had the most diverse (29 taxa) macroplankton community and the highest mean abundance (15 ind m^{-2}) (Table 1). *S. thompsoni* was the dominant species accounting for 82% of total abundance (Table 1). This was followed by euphausiids (9%), mostly *E. triacantha* and *E. vallentini*, and chaetognaths (~4%) (Table 1).

Comparison of macroplankton in eddies A and B

Total macroplankton abundance, although being similar between anticyclonic eddies A and B, was 1.8–2-fold higher at stations occupied outside than inside them (Table 2). Furthermore, stations occupied south of the APF showed significantly lower macroplankton abundance (almost sixfold) compared with all stations occupied north of the front (Table 2). A similar pattern was observed for *S. thompsoni* densities, except that their abundance inside eddy B was significantly lower than outside eddy A (Table 2).

Table 2 Average macrozooplankton, micronekton and salp densities (ind m^{-2}, ±1SD) inside and outside eddies A and B as well as south of the APF during the DEIMEC II cruise

	Inside eddy A	Outside eddy A	Inside eddy B	Outside eddy B	South of the APF
Total macroplankton (ind m^{-2})	10.8 ± 0.7	20.5	9.0 ± 3.8	16.5 ± 2.3	2.3 ± 0.3
Salpa thompsoni (ind m^{-2})	9.1 ± 1.2	17.3	3.8 ± 0.2	13.0 ± 3.5	0.7 ± 0.2
Total fish (ind m^{-2})	0.19 ± 0.03	0.18	0.08 ± 0.07	0.09 ± 0.05	0.36 ± 0.28
Euphausiids + decapods (ind m^{-2})	0.8 ± 0.3	2.1	3.8 ± 2.7	1.5 ± 0.6	0.7 ± 0.4

Total fish density was the highest south of the APF and the lowest inside and outside of eddy B (Table 2). Total density of euphausiids and decapods was similar between stations inside eddy A and stations south of the APF (Table 2). It was also similar at stations outside both eddies (Table 2). Lastly, euphausiid and decapod abundance was the highest, ca. 1.8–2.5-fold, inside eddy B compared with the stations outside both eddies. Only stations inside eddy A and stations south of the APF had significantly lower densities (up to 4.8-fold) of euphausiids and decapods compared with all other stations (Table 2). Most of the plankton ranged in size from 5 to 55 mm (Fig. 7b). The patterns in the size structure of total plankton were similar between eddies, both inside and outside of them, and south of the APF.

Discussion

Ansorge et al. (*2006*) have demonstrated that intense eddies downstream of the South-West Indian Ridge can be effectively tracked, using altimetry, as they move downstream towards the vicinity of the Prince Edward Islands, their anomalous SSH signature decreasing continuously along their path. Specific anomalies identified as three eddies were studied during the DEIMEC II survey. Eddy A, a recently spawned anticyclone lying to the south of the APF and comprising of modified SASW; eddy B, an anticyclone lying between the SAF and the APF and typical of the APFZ; and eddy C, a cyclone west of the ridge and characteristic of the Antarctic zone. Concentrations of total and micro Chl-*a* between eddies were low and did not show a clear pattern. Although not statistically significant, a relationship between elevated Chl-*a* concentrations and waters with lower temperatures, indicative of Antarctic origin, was observed. The Chl-*a*/phaeopigment ratios, however, had a clear pattern indicating that the highest ratios were almost always associated with the anticyclonic eddies and/or with the APF that meandered across the sampling region. From the biological point of view, higher Chl-*a*/phaeopigment ratios are indicative of the healthier and more productive phytoplankton and could be explained by the intrusion of nutrients into the area. Overall, the two anticyclonic eddies A and B typically SASW were not very productive, they were dominated by small size phytoplankton and consequently hardly distinguishable from surrounding waters. Observed low phytoplankton concentrations could be attributed to the increased grazing by zooplankton. However, our data indicate that the potential grazing impact (as predicted from zooplankton densities) imposed by *S. thompsoni* populations and herbivorous euphausiids appeared to be significantly lower inside than outside of both eddies supporting higher Chl-*a*/phaeopigment (autotrophy/heterotrophy) ratios. Nevertheless, in the absence of information on the smaller zooplankton size fraction, this assumption remains inconclusive, especially given the fact that at the micro- and mesozooplankton level, standing stocks and grazing have previously been shown to be substantial in this region (see Bernard and Froneman *2002*, *2005*). Furthermore, the combination of higher Chl-*a*/phaeopigment ratios with low Chl-*a* standing stock observed in this study, besides grazing losses, might imply high vertical losses of phytoplankton due to sinking. The lack of the vertical structure in the Chl-*a* structure appears to support this suggestion.

Although previous studies have consistently observed low productivity in the region south-west of the Prince Edward Islands (e.g. Bernard and Froneman *2002*, *2005*), it has been suggested that mesoscale eddies formed at the South-West Indian Ridge carry with them organisms from their region of origin so that the surrounding

waters of the Prince Edward Islands have a much more diverse spectrum of biota than one would normally expect from an island in the Subantarctic (Bernard et al. *2007*). Moreover, these eddies create unusual habitats of their own, particularly at their borders. This has become evident by the preferential foraging ground for top predators, such as the grey-headed albatross (Nel et al. *2001*). It has been documented on numerous occasions (Griffiths and Brandt *1983*; Pakhomov and Perissinotto *1997*; Bernard et al. *2007*; Strzelecki et al. *2007*) that the biomass and productivity of eddies may depend on the origin of water entrained into the feature. It also appears that the composition of larger plankton and micronekton may represent a better index for the eddy origin as they life cycle generally longer than the eddy life span (Griffiths and Brandt *1983*; Wiebe and Flierl *1983*; Wiebe et al. *1976*).

Macrozooplankton and micronekton communities have been separated into three distinct groups. South of the APF, an Antarctic community was observed. Typical Antarctic indicator species included euphausiids *E. frigida* and *E. triacantha*, the amphipod *Mimonectes sphericus* and the myctophid *Electrona antarctica* (Table 1). The remaining two groups, indicative of the community structure within eddies A and B, showed a distinct mix of sub-Antarctic species with either subtropical, as in the case of eddy B, or Antarctic (eddy A) indicator species. As expected, the size structure of total macroplankton/micronekton only showed significant differences between stations occupied north and south of the APF. The tunicate *S. thompsoni* is known to be a fast growing species (Foxton *1966*) that may mask differences in the community size structure. Major taxonomic groups, total plankton, as well as tunicates appeared to be more numerous outside of both eddies A and B than inside them (see Table 2). However, there were no significant differences between eddies A and B in total macroplankton and micronekton abundance. Furthermore, although there were no differences in fish densities across each eddy, average densities of fish within eddy A were more than double those within eddy B (Table 2). In addition, within eddy A, myctophids on average were bigger than in eddy B [65 ± 2.4 mm ($n = 12$) vs. 51 ± 8.3 mm ($n = 8$)], pointing to an even higher discrepancy between eddies in terms of fish biomass. On the other hand, the euphausiid density was substantially lower (0.8 ind m^{-2}) inside eddy A than in eddy B (3.8 ind m^{-2}, see Table 2). Thus, it appears that fish-preying top predators, such as the grey-headed albatross (Nel et al. *2001*), could have found better foraging grounds within eddy A. In contrast, crustacean preying top predators (several species of petrels) could have benefited more by foraging within eddy B.

The main aim of the DEIMEC II study was to investigate the physical and biological dynamics of eddies upstream of the Prince Edward Islands under the assumption that these eddies represented different stages in ageing in their downstream progress. Water mass characteristics confirm that the SSH anomaly A was indeed a recently spawned eddy from north of the APF composed of modified SASW. Anomaly B, at the time of the survey, was perceived to be an eddy of more advanced age and was composed of water masses more representative of true SASW and typical of the APFZ. Biogeographically, however, the two eddies were distinctly different in their origin and cannot, therefore, be treated simply as a 'new' and 'aged' eddies. Closer examination of their trajectories leading up the survey period (Fig. 1) clearly confirms that eddy B had been formed within the northern part of the APFZ and thus its water masses, comprising modified SASW, are typical of the transitional character of the Polar Frontal Zone (PFZ). The species composition within eddy B was different from the typical APFZ communities due to the presence of subantarctic and subtropical species in it, pointing to the close interactions with the SAF and Subantarctic Zone to the north. Furthermore, particulate organic matter stable isotope analyses confirmed this distinction (Kaehler and Pakhomov; unpublished data), suggesting that eddy B, instead of being a predecessor of eddy A, may have originated much further north and possibly even north of the SAF. The communities in eddy A were similar in composition to typical APFZ communities with the addition of some Antarctic species suggesting an origin just north of the APF. Indeed, underway measurements enroute to eddy A confirmed that that the APF lay close to its northern boundaries (Fig. 4b). This conclusion is also further supported by its water mass composition. The results of DEIMEC II highlight the role eddy features may have in this region in "relocating" macroplankton communities from one zone to another.

References

Ansorge IJ, Lutjeharms JRE (2003) Eddies originating from the South-West Indian Ridge. J Mar Syst 39:1–18

Ansorge IJ, Lutjeharms JRE (2005) Direct observations of eddy turbulence at a ridge in the Southern Ocean. Geophys Res Lett 32:L14603.

Ansorge IJ, Lutjeharms JRE, Swart N, Durgadoo JV (2006) Observational evidence for a cross frontal heat pump in the Southern Ocean. Geophys Res Lett 33:L19601.

Belkin IM, Gordon AL (1996) Southern Ocean fronts from the Greenwich meridian to Tasmania. J Geophys Res 101:3675–3696

Bernard KS, Froneman PW (2002) Mesozooplankton community structure in the Southern Ocean upstream of the Prince Edward Islands. Polar Biol 25:597–604

Bernard KS, Froneman PW (2005) Trophodynamics of selected mesozooplankton in the west-Indian sector of the Polar Frontal Zone, Southern Ocean. Polar Biol 28:594–606

Bernard ATF, Ansorge IJ, Froneman PW, Lutjeharms JRE, Bernard KS (2007) Entrainment of Antarctic euphausiids across the Antarctic Polar Front by a cold eddy. Deep Sea Res Part I 54:1841–1851

Boden BP (1988) Observations of an island mass effect in the Prince Edward Archipelago. Polar Biol 9:1–8

Budillon G, Rintoul SR (2003) Fronts and upper ocean thermal variability south of New Zealand. Antarct Sci 15:141–152

Clarke KR, Warwick RM (1994) Change in marine communities: an approach to statistical analysis and interpretation, 1st edn. Plymouth Marine Laboratory, Natural Environmental Research Council, Plymouth, pp 1–144

Field JG, Clarke KR, Warwick RM (1982) A practical strategy for analysing multi species distribution patterns. Mar Ecol Prog Ser 8:37–52

Foxton P (1966) The distribution and life-history of *Salpa thompsoni* Foxton with observations on a related species, *Salpa gerlachei* Foxton. Discov Rep 34:1–116

Froneman PW et al (2003) Physical and biological variability in the Antarctic Polar Frontal Zone: Report on the research cruise 104 of the M.V. S.A. Agulhas. S Afr J Sci 98:534–536

Gille ST (2003) Float observations of the Southern Ocean. Part II: Eddy fluxes. J Phys Oceanogr 33:1182–1196

Griffiths FB, Brandt SB (1983) Mesopelagic crustacean in and around a warm-core eddy in the Tasman Sea off eastern Australia. Aust J Mar Freshwat Res 34 (4):609–623

Gründlingh ML (1995) Tracking eddies in the southeast Atlantic and southwest Indian oceans with TOPEX/Poseidon. J Geophys Res 100:24977–24986

Koshlyakov MN, Grachev YM, Sazhina TG, Yaremchuk MI (1985) Cyclonic eddies in the region of the Antarctic circumpolar current and heat transfer across the Antarctic front. Okean 25:885–895

Lutjeharms JRE (1985) Location of frontal systems between Africa and Antarctica: some preliminary results. Deep Sea Res 32:1499–1509

Lutjeharms JRE, Baker DJ (1980) A statistical analysis of the meso-scale dynamics of the Southern Ocean. Deep Sea Res 27:145–159

Lutjeharms JRE, Valentine HR (1984) Southern Ocean thermal fronts south of Africa. Deep Sea Res 31:1461–1476

Nel DC, Pakhomov EA, Lutjeharms JRE, Ansorge IJ, Ryan PG, Klages NTW (2001) Exploitation of mesoscale oceanographic features by grey-headed albatrosses *Thalassarche chrysostoma* in the southern Indian Ocean.

Mar Ecol Prog Ser 217:15–26

Pakhomov EA, Perissinotto R (1997) Mesozooplankton community structure and grazing impact in the region of the Subtropical Convergence south of Africa. J Plankton Res 19:675–691

Pakhomov EA, Froneman PW, Ansorge IJ, Lutjeharms JRE (2000) Temporal variability in the physico-biological environment of the Prince Edward Islands (Southern Ocean). J Mar Syst 26:75–95

Park Y-H, Charriaud E, Poisson A (1997) Hydrography and baroclinic transport between Africa and Antarctica on WHP Section I6. Int WOCE Newsl 29:13–16

Pollard RT, Read JF (2001) Circulation pathways and transports of the Southern Ocean in the vicinity of the Southwest Indian Ridge. J Geophys Res 106:2881–2898

Pollard RT, Venables HJ, Read JF, Allen JT (2007) Large-scale circulation around the Crozet Plateau controls an annual phytoplankton bloom in the Crozet Basin. Deep Sea Res Part II 54:1915–1929

Robertson AA, Alexander DGW, Miller DGM (1981) Modified collapsible opening and closing midwater trawls (RMT-8 and RMT-2). Fish Bull S Afr 14:103–113

Roe HSJ, de C Baker A, Carson RM, Wild R, Shale DM (1980) Behaviour of the Institute of Oceanographic Science's rectangular midwater trawls: theoretical aspects and experimental observations. Mar Biol 56:247–259

Schulman E (1975) A study of topographic effects. In: Numerical Models of ocean circulation, National Academy of Science, Washington, pp 147–165

Sclater JG, Grindlay NR, Madsen JA, Rommevaux-Jestin C (2005) Tectonic interpretation of the Andrew Bain transform fault: Southwest Indian Ocean. Geochem Geophys Geosyst 6:Q09K10.

Strickland JDH, Parsons TR (1968) A practical handbook of seawater analysis. Fish Res Board Can 167:1–311

Strzelecki J, Koslow JA, Waite A (2007) Comparison of mesozooplankton communities from a pair of warm- and cold-core eddies off the coast of Western Australia. Deep Sea Res Part II 54:1103–1112

Swart NC, Ansorge IJ, Lutjeharms JRE (2008) Detailed characterization of a cold Antarctic eddy. J Geophys Res 113:C01009.

Wiebe PH, Flierl GR (1983) Euphausiid invasion/dispersal in Gulf Stream cold-core rings. Aust J Mar Freshw Res 34:625–652

Wiebe PH, Hulburt EM, Carpenter EJ, Jahn AE, Knapp GP, Boyd SH, Ortner PB, Cox JL (1976) Gulf Stream cold core rings: large-scale interaction sites for open ocean plankton communities. Deep Sea Res 3:695–710